Miner Deposita (2010) 45:23–41
DOI 10.1007/s00126-009-0256-0

ARTICLE

Magnetic polarity zonation within the El Teniente copper–molybdenum porphyry deposit, central Chile

Natalia Astudillo · Pierrick Roperch · Brian Townley · Cesar Arriagada · Annick Chauvin

Received: 31 May 2008 / Accepted: 29 July 2009 / Published online: 21 August 2009

Abstract El Teniente porphyry copper deposit, the world's greatest intrusion-related Cu–Mo ore body, is hosted within basaltic–andesitic volcanic and gabbroic rocks (mafic complex). This ore body is strongly affected by multiple events of alteration/mineralization with pervasive potassic and chloritic alteration and coetaneous with associated copper mineralization. We present paleomagnetic results obtained from oriented samples at four locations within the mine and from two drill cores, 200 and 400 m long, respectively. Samples are representative of all the main hydrothermally altered rock units, with emphasis on the mafic host rock and dacitic (Teniente dacite porphyry) and dioritic porphyry intrusions. Magnetic experiments [hysteresis loop, isothermal remanent magnetization (IRM), *k*–*T* curves, thermal, and alternating field demagnetization] show the presence of prevailing magnetite. Microscope and SEM observations show two families of magnetite, (a) large multidomain magnetite grains, associated with biotite and chlorite of various different hydrothermal alteration events, and (b) abundant small to medium grain-size magnetite (<10 μm) contained within plagioclase, either related to an early Na–Ca–Fe alteration or included within plagioclase during magmatic crystal growth. While the Teniente dacite porphyry and the quartz diorite–tonalite have low magnetic susceptibility (<0.0005 SI) and low natural remanent magnetization (NRM, 10^{-4}–10^{-3} Am^{-1}), the mineralized mafic host rocks have usually high susceptibility (>0.01 and up to 0.2 SI) with NRM in the range 0.1–2 Am^{-1}. Most mafic complex rock samples have univectorial magnetizations during alternating field or thermal demagnetization. Within the mine, the magnetic polarity is spatially distributed. In the northern part of the deposit, the Teniente dacite porphyry, the associated hydrothermal breccias, and the hosting mafic complex record a reverse polarity magnetization, also observed in the El Teniente sub-6 mine sector immediately to the east and southeast. In the eastern part of the deposit, a normal polarity is observed for samples of the mafic complex from the two long drill cores. There is no evidence for superimposed magnetizations of opposite polarities in samples of the mafic complex. Anhysteretic remanent magnetization (ARM) in a DC field of 40 μT and NRM have similar magnitude and comparable behavior upon alternating field demagnetization. The well-defined strong remanent magnetizations associated with high unblocking temperatures (>500°C) indicate an acquisition of remanent magnetization during mineralization by circulating high temperature fluids related with ore deposition. Paleomagnetic results and the recorded polarity zonation suggest multiple mineralization events occurred at El Teniente, each one with its own evolution

Editorial handling: F. Tornos

Electronic supplementary material The online version of this article (doi:10.1007/s00126-009-0256-0) contains supplementary material, which is available to authorized users.

N. Astudillo · B. Townley · C. Arriagada
Departamento de Geología,
Facultad de Ciencias Físicas y Matemáticas,
Universidad de Chile,
Plaza Ercilla 803,
Santiago, Chile

N. Astudillo · P. Roperch (✉)
LMTG, IRD, Université Paul Sabatier Toulouse III,
14 Av. E. Belin,
31400 Toulouse, France
e-mail: pierrick.roperch@ird.fr

P. Roperch · A. Chauvin
Géosciences Rennes, Université de Rennes 1,
Campus de Beaulieu,
35042 Rennes, France

stages, superimposed within the district. These results indicate that a simplified broad four-stage model for El Teniente, as presented and overly employed by many authors, divided in (1) late magmatic, (2) main hydrothermal, (3) late hydrothermal, and (4) posthumous stage, does not recognize various short-lived single mineralization events, some superimposed and some distinctly separated in time and space. There is no paleomagnetic evidence for post-mineralization deformation

Keywords Paleomagnetism · Magnetic polarity · El Teniente · Porphyry copper · Chile

Introduction

Numerical models suggest that cooling of magmatic-hydrothermal systems occurs within short periods of time, often within the resolution range (<100 ka) of the majority of the geochronologic methods (Cathles et al. 1997; Seedorff et al. 2005). In porphyry copper deposits, subvolcanic intrusions represent apophyses of deeper magmatic chambers which exsolve hydrothermal fluids enriched in metal elements such as copper (Dilles and Einaudi 1992). In porphyry copper systems, high temperature mineralization processes are commonly short lived as compared to the much longer low temperature cooling evolution associated in part with deep circulation of meteoric water (Hedenquist and Richards 1998). The history of cooling of large hydrothermal systems may be deciphered by use of complementary isotopic-age determinations such as the U–Pb, Re–Os, and $^{40}Ar/^{39}Ar$ methods. Even if radiochronological studies show that the duration of the magmatic-hydrothermal activity in some deposits can be very short, significant differences (1–2 Ma) are sometimes observed between the U–Pb ages on zircon of the intrusions and $^{40}Ar/^{39}Ar$ ages on hydrothermal biotite (e.g., El Teniente, Maksaev et al. 2004; Escondida, Padilla-Garza et al. 2004; Río Blanco, Deckart et al. 2005; and Bajo de la Alumbrera, Harris et al. 2008). Within the large porphyry deposits characterized by multiple intrusions, differences in ages are often attributed to superimposed phases of mineralization occurring during a time interval longer than 1 Ma.

An interpretation in terms of cooling can however be complicated by the systematic differences sometimes observed among age data resulting from different isotopic systems. These differences may be attributed to times of residence of several 100 ka of zircon in the magma (Reid et al. 1997), to an uncertainty in the constant decrease of ^{40}K (Palfy et al. 2007), disturbance of the isotopic systems due to reheating or gas loss, existence of inherited cores in zircon, among many others.

Magnetostratigraphy, in favorable circumstances, can be an interesting complement to better constrain the ages obtained by radiometric dating. For example, paleomagnetic studies decisively demonstrated the short duration of emplacement of the large volcanic plateaus like the Deccan flood basalts (Courtillot et al. 1988).

The history of magnetic minerals during processes of mineralization is however likely complex and few paleomagnetic studies have been applied to hydrothermal systems (Townley et al. 2007; Alva-Valdivia et al. 2003). For example, paleomagnetism was used to date some old deposits by comparison of the observed paleomagnetic poles with the expected apparent polar wander path (Symons et al. 2002; Symons and Arne 2005). In non-altered volcanic rocks or intrusive rocks, natural remanent magnetization (NRM) is mainly a thermoremanent magnetization and is recorded at the time of cooling below the Curie temperature of the magnetic minerals in the rocks (580°C for magnetite). During strong hydrothermal alteration, remagnetization by heating, destruction, or formation of new magnetic minerals may occur during the circulation of the hydrothermal fluids at temperatures sometimes lower than the Curie temperatures of magnetite. If it is possible to isolate well-defined components of remanent magnetization, paleomagnetism is then likely to bring additional information to the isotopic dating methods.

El Teniente is a typical porphyry Cu–Mo deposit—in terms of its alteration and sulfide assemblage zonation, association with the intrusion of quartz diorite–tonalite and dacite porphyries within subvolcanic and volcanic mafic host rocks, and predominance of quartz, biotite, and biotite–quartz–sericite–chlorite vein-hosted and disseminated copper mineralization. The world's largest known porphyry Cu deposit, it contains a total of >94 million metric tons (Mt) of fine copper. It is located in the Mio-Pliocene Andean cordillera of Central Chile, 70 km southeast of Santiago (Fig. 1). High-resolution radiogenic dating (Maksaev et al. 2004) have significantly improved our knowledge of the timing and duration of hydrothermal and magmatic activity of the El Teniente supergiant porphyry Cu–Mo deposit. Most of the mineralization is hosted within a mafic rock complex, including altered basalts, diabases, andesites, and related subvolcanic gabbros, originally referred to as the "Andesites of the mine," and currently named "Complejo Máfico El Teniente (CMET)" El Teniente mafic complex. Rocks of the CMET are intruded by the Teniente dacite porphyry and a number of quartz diorite to tonalite stocks of which the largest is the Sewell quartz diorite–tonalite intrusion in the southeastern section of the deposit and the two smaller Northern and Central quartz diorite–tonalite bodies, located in the central north portion of the deposit (Fig. 2 and Electronic supplementary material, ESM Fig. 1).

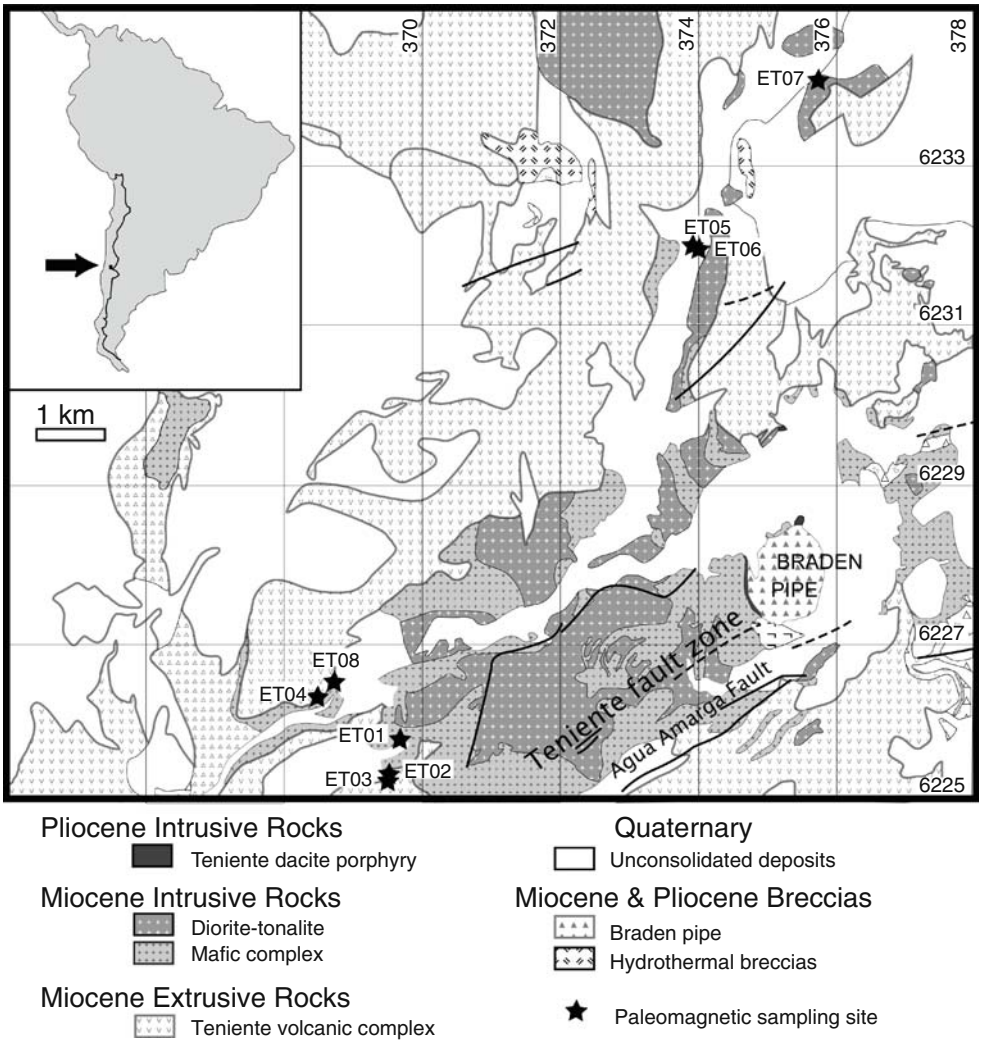

Fig. 1 Geological map of the El Teniente mine area and paleomagnetic sampling sites for samples from the Teniente volcanic complex outside the mine (modified from El Teniente Codelco map, provided by El Teniente Division of CODELCO-Chile and Skewes et al. (2005)) (map in UTM coordinates)

In addition, the CMET and Sewell quartz diorite–tonalite rocks are intruded by a fine grained quartz diorite stock, termed the A porphyry. While most authors attribute the mineralization to the intrusions of the Sewell stock, the Northern and Central quartz diorite–tonalite stocks, and the Teniente dacite porphyry (Maksaev et al. 2004), Skewes et al. (2005) argue that the mineralization within the andesites mostly occurred before the emplacement of the stock intrusions.

We have undertaken a detailed paleomagnetic study with the aim to bring possible new constraints on the timing of mineralization. Here, we report paleomagnetic results at several locations within the biotite-altered CMET rocks as well as within the Teniente dacite porphyry and quartz diorite–tonalite intrusions (Sewell, Central and Northern stocks). The stock intrusions and associated mineralization in the CMET mafic host rock encompass a time interval between 6.5 and 4.3 Ma (Maksaev et al. 2004), covering several geomagnetic polarity reversals.

Geology

Mineralization at El Teniente

Most of the mineralization is hosted within rocks of the CMET, composed of gabbros, diabases, and porphyritic basalts and basaltic andesites often correlated to the early to middle Miocene Farellones volcanic formation (Ossandón 1974; Camus 1975; Villalobos 1975; Cuadra 1986; Burgos 2002; Maksaev et al. 2004; among others) (Fig. 3).

The textural and geochemical features of rocks of the CMET have however been obscured by widespread, pervasive, texture destructive biotite alteration.

In agreement with Lindgren and Bastin (1922) and Skewes et al. (2002), Cannell et al. (2005) interpret the CMET rock sequence as a sill and stock complex of crystal-supported feldspar±hornblende-phyric to aphanitic andesite that intrudes andesitic lava flows and volcaniclastic units of the Farellones Formation. Although the age of the CMET is

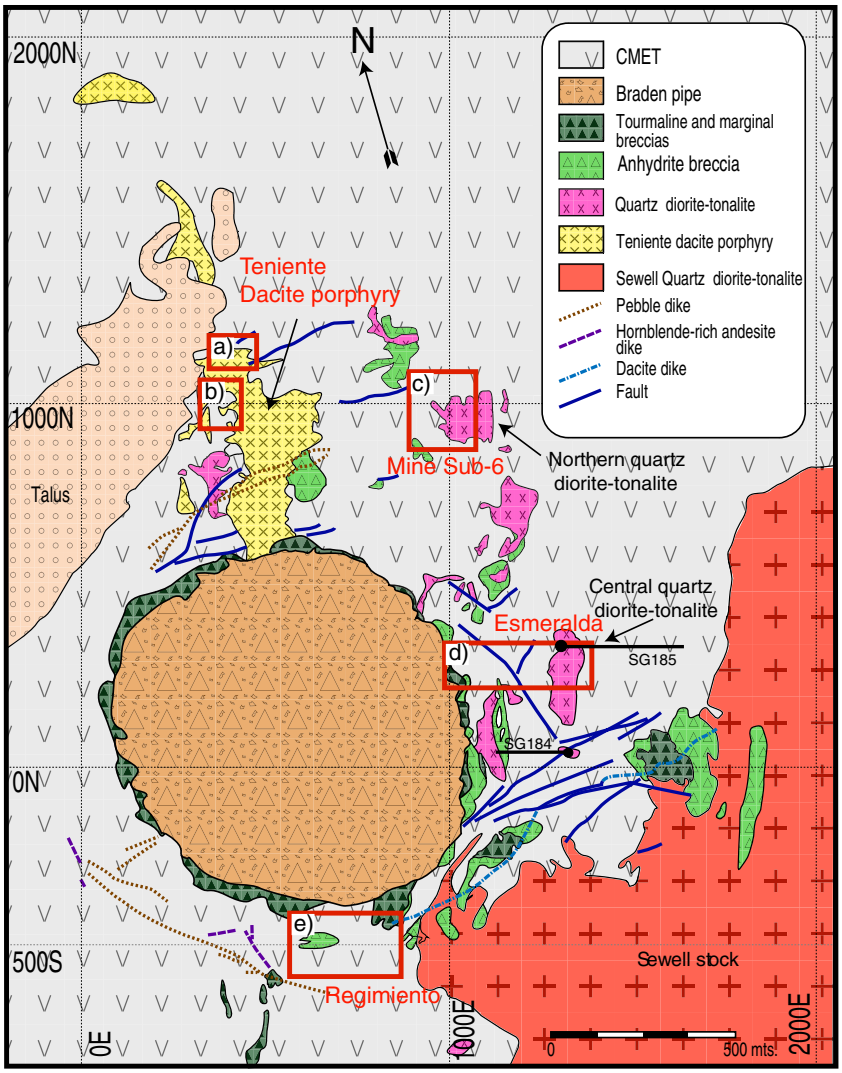

Fig. 2 Geology of the four LHD level (2,354 m) of the El Teniente mine (map provided by El Teniente Division of CODELCO-Chile). *Rectangles* represent sampling sites of oriented blocks (detailed maps in the Electronic supplementary material). The drill cores SG184 and SG185 are shown with *thick lines*. Scale in mine coordinates in meters

difficult to constrain because of the lack of primary minerals, Maksaev et al. (2004) interpret a fission track age of 8.9±2.8 Ma, from a mafic sill 5 km west of El Teniente, as an age of rapid cooling of the CMET.

The central part of the deposit is intruded by the Braden breccia pipe, a weakly mineralized phreatomagmatic polymictic tourmaline, and rock powder breccia that cuts the entire deposit.

Most authors (e.g., Camus 1975; Maksaev et al. 2004) indicate that there is an intimate spatial and temporal association between all stages of mineralization and the Late Miocene to Early Pliocene stock intrusions at El Teniente. Maksaev et al. (2004) report numerous new radiometric ages (U–Pb in zircons of the tonalite, diorite, and dacite intrusions, $^{40}Ar/^{39}Ar$ in biotite and sericite, and Re–Os in molybdenite). The oldest intrusives are the Sewell, Northern and Central quartz diorite–tonalite stocks and the A porphyry fine-grained quartz diorite in the eastern part of the deposit (6.46±0.11 to 6.11±0.13 Ma zircon U–Pb). A zircon U–Pb age of 5.28±0.10 Ma was obtained for the Teniente dacite porphyry, while the dacite-ring dikes related to the central Braden breccia pipe are slightly younger (zircon U–Pb age of 4.82±0.09 Ma; Maksaev et al. 2004).

In the most commonly adopted model for El Teniente (Cuadra 1986; Arevalo et al. 1998), the hydrothermal alteration and ore-forming processes take place during four main stages: (1) late magmatic, (2) main hydrothermal, (3) late hydrothermal, and (4) posthumous stage. According to this model, most of the copper was precipitated during the late magmatic stage (6.5–4.9 Ma), contemporaneously with intrusions of the quartz diorite–tonalite stocks and the Teniente dacite porphyry within rocks of the CMET. Mineralization of the late magmatic stage is mainly hosted by a quartz–anhydrite-dominated stockwork associated with selective pervasive potassic alteration (Kfeldspar and biotite) of the Teniente dacite porphyry and pervasive potassic alteration (biotite and Na-Kfeldspar) of the CMET

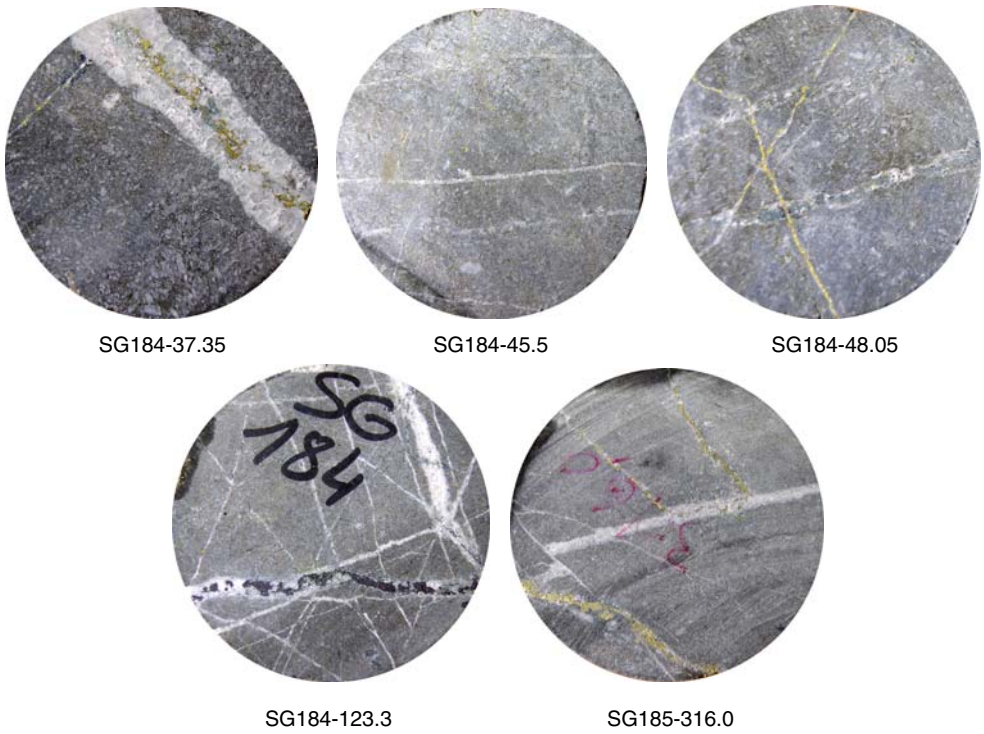

Fig. 3 Photographs of drill-core section (6 cm in diameter) of five samples from the El Teniente Mafic complex. These samples show a pervasive potassic biotite background alteration, cut by quartz–sericite, sericite–chlorite halo quartz–chalcopyrite veinlets, in some cases potassic alteration observing weak to moderate quartz–sericite alteration superimposition

rocks (Skewes et al. 2002, 2005; Maksaev et al. 2004; Cannell et al. 2005). Minor copper-mineralized hydrothermal biotite-cemented breccias are formed during this stage. The late magmatic stage was followed by two events of mineralized phyllic alteration, referred to as the principal hydrothermal (4.9–4.8 Ma) and late hydrothermal (4.8–4.4 Ma) stages, during which thicker, Cu-rich veins were emplaced. The Braden breccia pipe formed during the late hydrothermal stage and Cannell et al. (2005) indicate that a large amount of ore was destroyed from the center of the deposit during the emplacement of the 1,200-m-wide breccia pipe. The last hypogene alteration event occurred mostly within the Braden breccia pipe and includes anhydrite, siderite, and gypsum.

Cannell et al. (2005), on the basis of the composition of mineralized veins, have interpreted a pre-mineralization stage, related to partial replacement of plagioclase by fine-grained magnetite (<8 μm, Skewes et al. 2005; Fig. 4a, c, g, i) and veins of magnetite and actinolite, predominantly preserved in the margins of the CMET. In addition, Cannell et al. (2005) interpret the posthumous stage as part of the hydrothermal stage.

Adjacent to the deposit, there is a zone of transitional biotite–chlorite alteration with quartz–chlorite–anhydrite–pyrite veins and chlorite alteration of secondary biotite (Camus 1975; Skewes et al. 2002, 2005). Surrounding the deposit, a zone of propilitic alteration (Villalobos 1975; Camus 1975; Zuñiga 1982), with weak replacement of primary minerals by epidote–chlorite–calcite–hematite has been recognized. At surface, a zone of leaching and supergene enrichment occurs, with thicknesses between 100 and 500 m, controlled by the topography and the permeability of the Teniente dacite porphyry and the Braden breccia pipe.

In contrast with the most accepted model linking copper mineralization to hydrothermal fluids associated with the quartz diorite–tonalite and dacite intrusions, Skewes et al. (2005) argue that mineralization at El Teniente spanned a time period of >2 Ma, between >7.1 and 4.4 Ma, during which multistage emplacement of breccias and mineralization–alteration occurred coetaneous to the emplacement of the CMET. These authors argue that the amount of copper at El Teniente is too large to be associated with the small volume of the quartz tonalite–diorite and dacite stock intrusions. According to Skewes et al. (2005), the stocks cut both the mineralized breccias and their mafic intrusive host rocks and have truncated and redistributed pre-existing copper mineralization.

Tectonic and structural setting

The possible role of active tectonic structures controlling the location of the El Teniente deposit is still debated; yet, it bears importance regarding a paleomagnetic study. The emplacement of the El Teniente porphyry copper deposit occurred during a time of regional E–W shortening associated with the intersection of subvertical faults oblique to the continental margin. The Teniente fault zone (TFZ) is dextral, subvertical, of approximately 14 km in length and 3-km wide and trends NE–ENE (Garrido et al. 1994; Fig. 1). Four subvolcanic intrusive centers are aligned along

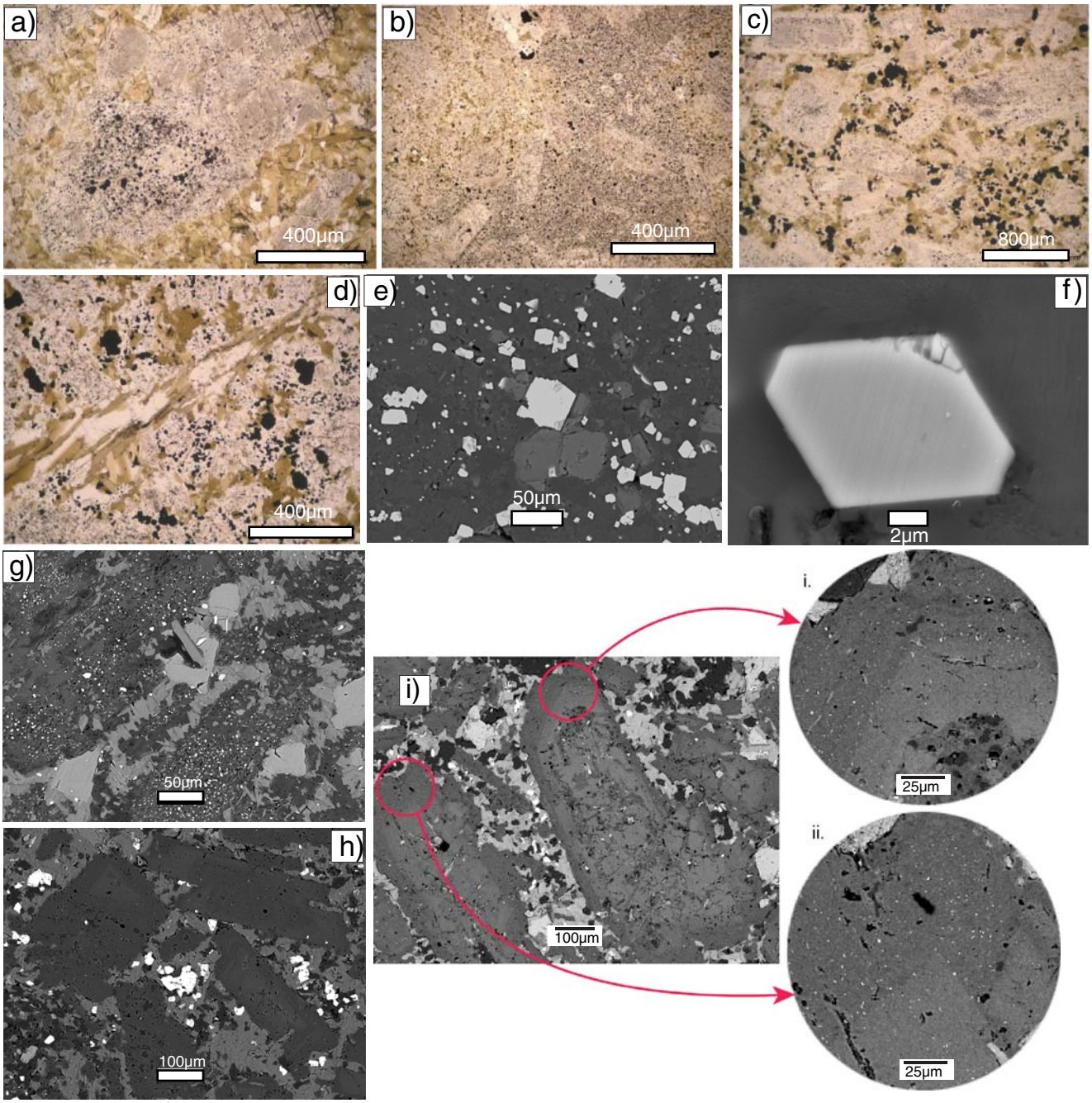

Fig. 4 Microphotographs of thin sections in samples from the El Teniente Mafic Complex. **a** Sample SG184-45.5: fine-grained magnetite crystals in plagioclase; these particular magnetite grains are not associated with the outer biotite potassic alteration of rock; **b** sample SG184-171.0: fine-grained magnetite associated with quartz and biotite in potassic altered groundmass of rocks. **c** Sample ETM1602 (mine sub-6): fine–grained magnetite in plagioclase and coarse-grained magnetite associated with biotite crystals of groundmass potassic altered host rock. Note that magnetite within plagioclase is different from groundmass biotite alteration related magnetite. **d** Sample SG184-222.45, same as in **c**; **e**, **f** sample ETM0302 (sub-6 mine sector): fine grained anhedral crystals of magnetite in plagioclase. **g** Sample ETM1501 (sub-6 mine sector): medium to fine-grained magnetite in potassic altered groundmass, **h** sample ETM1601: coarse grained magnetite in potassic altered groundmass; **i** sample ETM1602: very fine-grained magnetite in plagioclase rims. **a**–**d** Transmitted light. **e**–**i** backscatter SEM images

the TFZ. Garrido et al. (1994, 2002) suggest that the TFZ controls the location of the Sewell stock, slightly elongated along a NE direction, as well as later events of brecciation in the deposit.

Within the deposit, the largest structures (a few meters up to 30–40 m long) correspond to a set of subvertical fractures of N–S direction, similar to the Teniente dacite porphyry and the apophyses related to the Sewell stock

(Cuadra 1986). Another set of fractures is arranged concentrically to the Braden breccia pipe with up to 40 fractures and veinlets per meter in the proximity of the breccia pipe (Zúñiga 1982), these together with a secondary system of subvertical radial dikes and fractures. The smallest structures form a three-dimensional network of veins, faults, and joints (stockwork) with no preferential direction. Cannell et al. (2005) found no clear structural control to the different stages of hydrothermal alteration.

Sampling and analytical methods

The El Teniente mine is an underground mine where classic paleomagnetic sampling techniques like portable gasoline drill or solar azimuth orientation cannot be deployed. For this reason, only blocks oriented with a magnetic compass were taken from the wall of several tunnels at four different locations within the mine (Fig. 2 and ESM Fig. 1a–e; Teniente dacite porphyry, labels a and b; mine-sub-6 sector, label c; Esmeralda mine sector, label d; and Regimiento mine sector, label e). Taking into account the precise orientation of the tunnels used for mining operation, no large magnetic deviations were detected. However, errors in the magnetic orientation of each block because of the numerous metallic artifacts used to maintain tunnel's stability and the difficulty to orient blocks might likely exceed 5°. However, we believe that most of these errors are random and tend to average out. The location of each block was referenced with respect to the detailed mapping of the underground tunnels.

Four distinct sectors of the El Teniente mining district were sampled (Fig. 2 and ESM Fig. 1). Sixteen blocks were taken in the Teniente sub-6 sector (ESM Fig. 1c), 35 blocks in the Esmeralda sector (ESM Fig. 1d), 31 blocks in the Regimiento sector (ESM Fig. 1e), and 16 blocks in the Teniente dacite porphyry (Fig. 2 and ESM-Fig. 1a, b). One or two 1-in. cores were later drilled from the selected blocks and oriented following the original orientation of the block.

Drill cores from underground mine boreholes were also sampled (Fig. 2; 24 standard minicores over a 190-m depth interval for SG184 with a plunge of 45° toward the west and 115 standard minicores over a 400-m depth interval for SG185 with a 45° plunge toward the east).

Finally, eight sites at surface were also drilled to the west and to the north of the mine (Fig. 1) in volcanic rocks from the Teniente volcanic complex, these to evaluate the existence of tectonic rotations.

A total of 299 paleomagnetic samples span the entire deposit, from surface to all current mines and deeper drill cores, these samples providing adequate and representative coverage of the deposit within accessible areas of an active underground mine.

Paleomagnetic samples were processed following standard paleomagnetic procedures, and the reader is referred to Butler (1992) or Tauxe et al. (2009) for excellent introductory books on paleomagnetism.

All samples were later cut to standard samples of 2.2 cm, properly marked and prepared for paleomagnetic measurements. NRM for each sample was measured with Spinner type magnetometers either with the Molspin (10^{-4}–500 A/m) or Agico JR5A (10^{-5}–1,500 A/m) at the paleomagnetic laboratory of the Department of Geology, University of Chile–IRD collaborative, in Santiago. Drill core samples from bore hole SG185 were all measured with a new 2G cryogenic magnetometer at the paleomagnetic laboratory of Rennes, France and demagnetized by alternating field (AF) with the 2G online demagnetizer. Additionally, volumetric magnetic susceptibility (k) was measured with a Bartington susceptibility meter.

In general, one or two specimens from each paleomagnetic core were subjected to progressive demagnetization either thermal or with the AF method. IRM were given in field up to 1,200 mT with an ASC pulse magnetizer. Curie temperatures were determined with the Agico kappabridge (KLY3S) and associated CS3 furnace at the University of Chile.

To assess the nature of the NRM, ideally, the NRM should be compared with a laboratory thermoremanent magnetization (TRM) acquired in a known DC field. Unfortunately, the magnetic mineralogy of a mineralized rock is likely to be modified upon heating in the laboratory. Since ARM mimic the properties of TRM without the need of heating the sample up to the Curie point of magnetite (580°C; with the consequent risk of a significant mineralogical modification), ARM was measured at room temperature in a DC field of 40 μT under an AC field of 110 mT using the 2G AF demagnetizer at Rennes.

Acquisition of a laboratory chemical remanent magnetization (CRM) during heating was performed on samples showing large increase in magnetic susceptibility upon heating in the laboratory. The samples were heated in a DC field of 40 μT and kept at 450°C or 460°C during 3 h and then cooled to room temperature in zero field.

Paleomagnetic results

Magnetic properties

Most samples from the Teniente dacite porphyry and Quartz diorite–tonalite stocks have magnetic susceptibility lower than 10^{-4} SI and NRM in the range 10^{-4}–10^{-3} Am^{-1} (Fig. 5). In rocks of the CMET, most samples (Fig. 5) have magnetic susceptibility above 10^{-2} SI with a few samples above 10^{-1} SI, while samples with the lowest magnetic

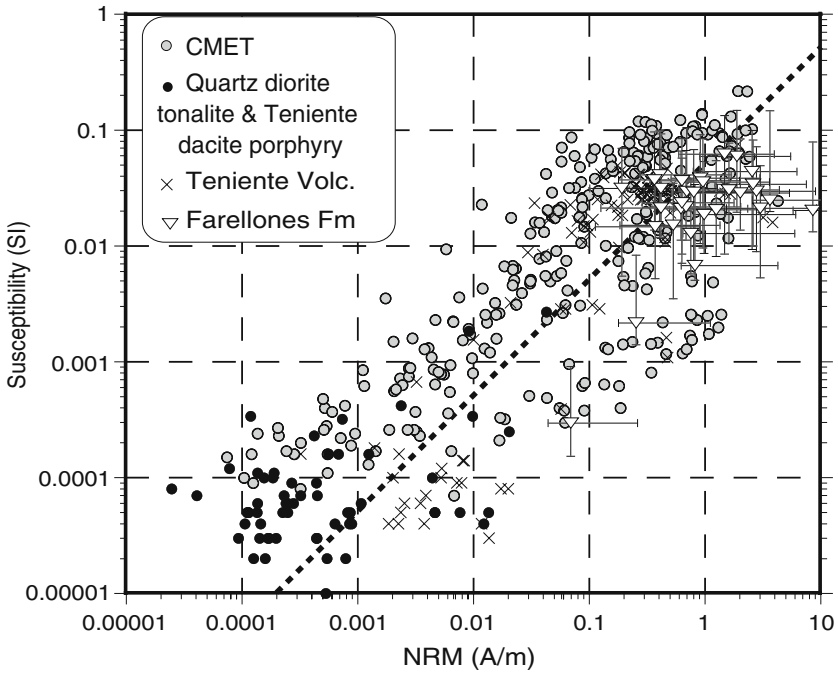

Fig. 5 Log–log plot of magnetic susceptibility versus intensity of NRM for all samples in the ore body. Altered rocks are compared with country rocks of the Teniente volcanic complex (*crosses*) and Farellones Formation (*triangles*). Samples from the intrusive stocks (Teniente dacite porphyry and quartz diorite–tonalite intrusions) have low magnetic susceptibility, while the mineralized mafic rocks have high magnetic susceptibility similar or higher than the Farellones volcanics. The lowest magnetic susceptibility values in the CMET correspond to samples with phyllic alteration. Data for the Farellones formation represent sampling site mean values from Goguitchaichvili et al. (2000)

susceptibility and NRM intensity show strong phyllic alteration (Figs. 5 and 6a). Magnetic susceptibility can reach higher values in the CMET rocks than in non-mineralized rocks of the Farellones (Goguitchaichvili et al. 2000) and Teniente volcanic complex Formation (Fig. 5).

The magnetic contrast between the intrusive rocks and rocks of the CMET is sharper along the drill core SG185 (Fig. 6) than along the Esmeralda E–W profile, possibly because the sampling of the drill cores SG184 and SG185 was slightly biased toward core pieces with a more mafic composition and possibly less quartz–sericite alteration.

All the thermomagnetic experiments in samples of the CMET indicate pure magnetite as the main magnetic mineral present in these rocks (Fig. 7a and ESM Fig. 2). During thermal demagnetization, dacite and quartz diorite–tonalite stock samples and some of the hydrothermal breccia samples with low initial magnetic susceptibility observe a large increase in magnetic susceptibility after heating above 400°C (ESM Fig. 2). The increase in magnetic susceptibility is related to the formation of magnetite above 400°C. It was not possible to determine the characteristic direction after thermal demagnetization above 400°C for most samples with low NRM ($<10^{-3}$ Am^{-1}) and low magnetic susceptibility; this is due to the acquisition of a spurious component of remanent magnetization in the laboratory associated with the formation of laboratory grown new magnetite crystals (see also the experiments on CRM acquisition). Samples from the mafic rocks with high initial magnetic susceptibility (>0.01 SI) do not show major changes in magnetic susceptibility after heating in the laboratory up to 580°C (ESM Fig. 2), and the characteristic direction was easily determined during progressive thermal demagnetization.

IRM acquisition in samples from the CMET show complete saturation above 250 mT, while saturation is not always attained for samples with low magnetic susceptibility (Fig. 7b). Back-field demagnetization of saturation IRM (ESM Fig. 3) provide evidence for relatively high Hcr values (>20 mT) for some samples suggesting the possible contribution of single domain or pseudo-single domain magnetite grains in agreement with optical and SEM observations showing numerous small grains of magnetite in plagioclase minerals (Fig. 4). For a few samples, medium destructive AF field (MDF) values above 100 mT and non-saturation of IRM above 300 mT indicate the contribution of high coercive minerals, possibly hematite. Hysteresis experiments in CMET samples show low Jrs/Js values with multidomain magnetite dominating the magnetic signal (ESM Fig. 3).

Characteristic directions

Teniente dacite porphyry (ESM Fig. 1a, b) Despite very low NRM intensity, several samples exhibit well-defined characteristic component in the course of the thermal or AF demagnetization (Fig. 7c and ESM Fig. 4). The magnetization is of reverse polarity (Fig. 8a) in the Teniente dacite porphyry and in the CMET nearby country rocks.

Mine sub-6 sector (ESM Fig. 1c) Samples from the Northern quartz diorite–tonalite have low magnetization

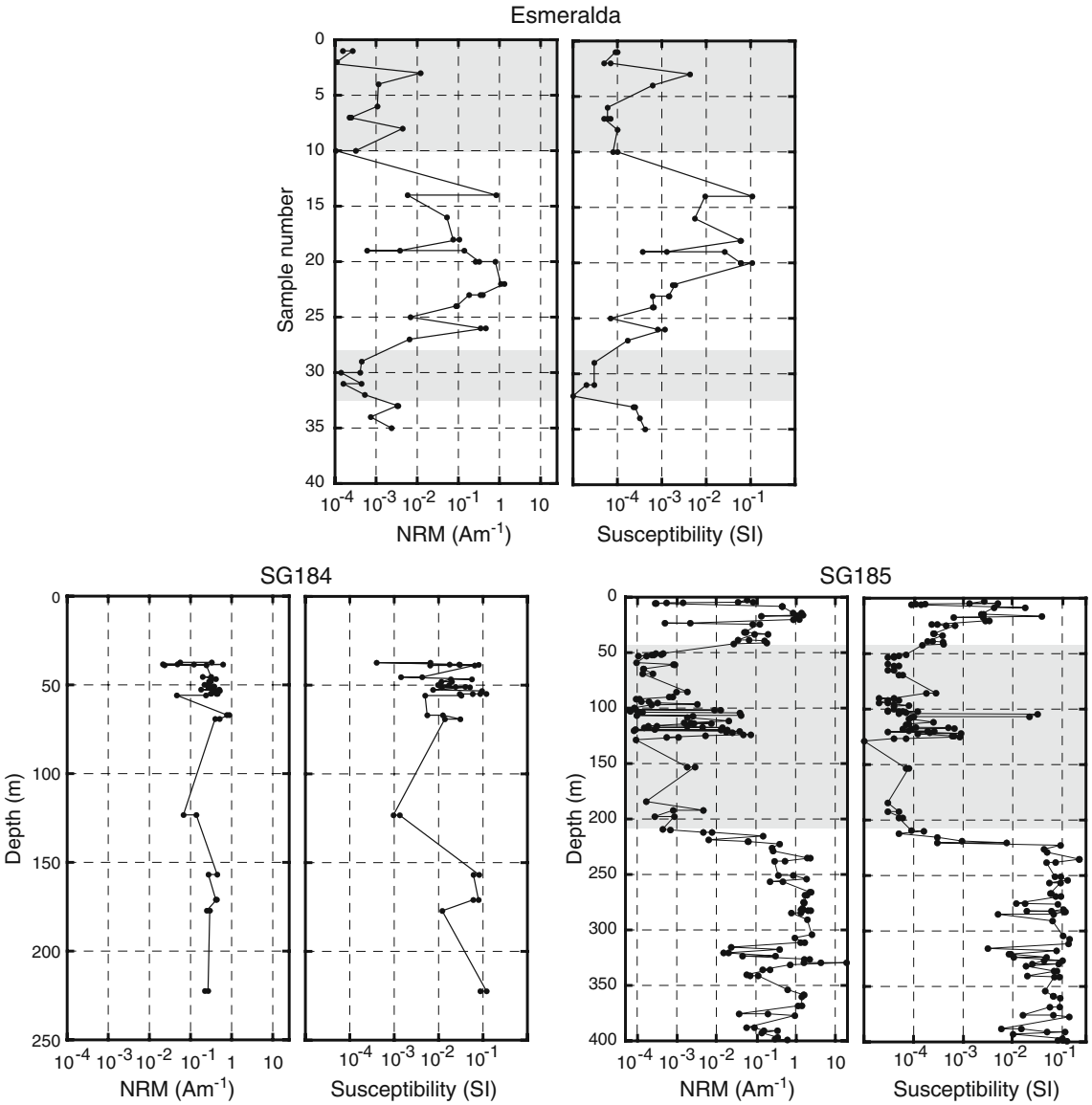

Fig. 6 *Top* Plots of NRM intensity and susceptibility variation along the Esmeralda profile from east to west. *Bottom* Plots of NRM intensity and susceptibility variation versus depth for drill cores SG184 and SG185. The *light gray shadow zone* corresponds to quartz diorite–tonalite rocks. The other samples are in the CMET

and low magnetic susceptibility (about 10^{-4} SI), and it was not possible to isolate a characteristic magnetization. In contrast, samples within the breccia or within the CMET have a stable reverse polarity magnetization (ESM Fig. 4 and Fig. 8b).

Regimiento mine sector (ESM Fig. 1e) In Regimiento, both magnetic polarities are found. The samples closest to the Braden breccia pipe (TR01–TR06) or the Sewell stock (samples TR12–TR27) have magnetization with intensity lower than 0.1 A/m and normal polarity. In contrast, samples TR07–TR11 located within 30 m (ESM Fig. 1e) have a well-defined characteristic magnetization with reverse polarity carried by magnetite (Fig. 8c). Some samples from this group with reverse polarity have the highest intensity of remanent magnetizations, above 0.1 A/m.

Esmeralda mine sector (ESM Fig. 1d) The sampling corresponds to a 350-m profile between the Braden breccia pipe and a dioritic stock. All samples within and nearby the contact with the intrusive stocks have low magnetization (Fig. 6), and it is not possible to clearly define a stable component of magnetization. A characteristic direction was determined in 11 samples (Fig. 8d). Only one has a reverse polarity magnetization (sample ETE08, ESM Fig. 4).

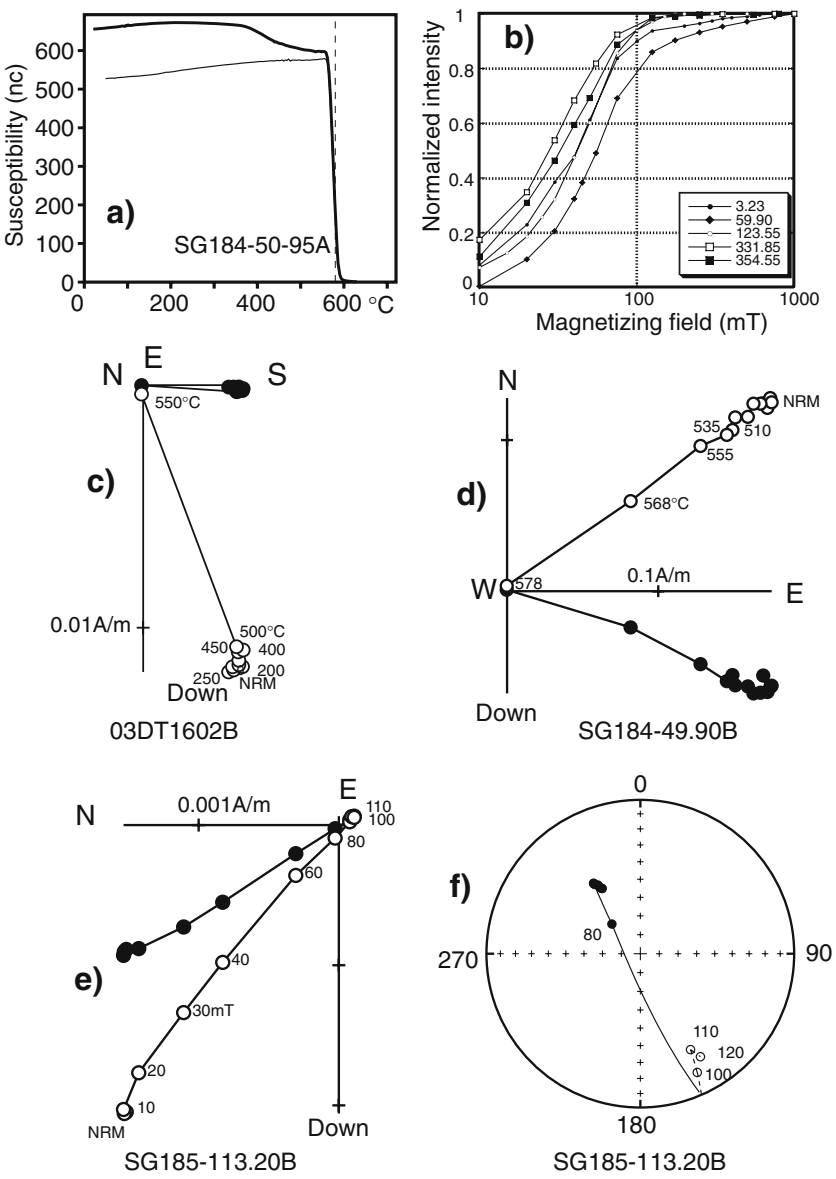

Fig. 7 Magnetic properties. **a** Example of a thermomagnetic experiment (susceptibility in arbitrary unit not normalized to volume or mass) showing magnetite as the main magnetic mineral with a Curie temperature of 580°C. **b** Acquisition of isothermal remament magnetization in different samples from drill core SG185. Except in two samples, saturation is usually observed below 250 mT in agreement with magnetite as the main magnetic carrier. **c**–**e** Examples of orthogonal diagram of progressive thermal (**c**, **d**) or alternating field (AF) demagnetizations (**e**). *Open (filled) symbols* are respectively projection of the vertical (horizontal) component of magnetization. **f** Equal area projection of the magnetic vector during demagnetization of the sample SG185-113.20B. During AF demagnetization an opposite polarity is observed above 80 mT. Samples SG184-49.90B and SG185-113.20B are shown in drill core coordinate. Sample 03DT1602B of the Teniente dacite porphyry is shown in in situ coordinate. Additional examples of magnetic properties and demagnetization plots are shown in Electronic supplementary material

Drill core SG0184 All but five samples have magnetization intensity between 0.1 and 1 A/m (Fig. 6). During thermal and AF demagnetization, a single component of magnetization is observed. Unblocking temperatures in the temperature range 500–580°C (Fig. 7d and ESM Fig. 5) and MDF values above 30 mT indicate that the characteristic magnetization is carried by single domain or pseudo-single domain magnetite. All the characteristic directions have the same negative inclination in drill core coordinates (Fig. 11a). Taking into account the orientation of the drill core (269° and 45°), the magnetization is of normal polarity.

Drill core SG185 Except in the depth interval corresponding to the Central quartz diorite–tonalite stock, which is where the magnetization is low ($<10^{-3}$ A/m), most samples have high magnetization with several values above 1 A/m (Fig. 6). A characteristic direction was identified after AF and thermal demagnetization in most samples from this drill core, especially in the CMET samples (ESM Fig. 5). Within the drill core SG185, there is evidence of a vertical zonation of the MDF values with low MDF values in the depth interval 220–260 m and high MDF from 260 to 300 m (Fig. 9). These variations in MDF values reflect magnetite grain size variation with low MDFs indicating more multidomain grains. It is unclear whether this magnetic variation is related to changes in lithology of the country rock prior to mineralization or to a different type of alteration. Samples from the CMET with NRM intensity above 1 A/m have, in most cases, MDF values above

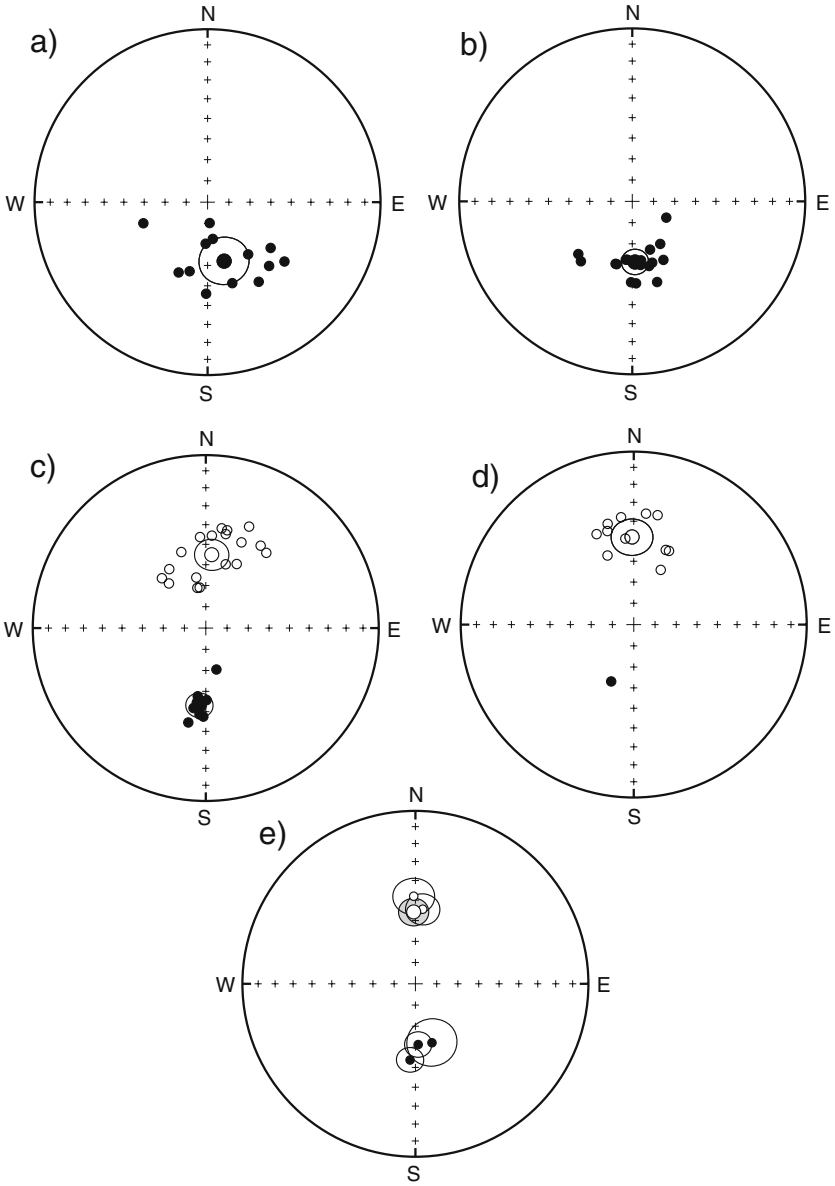

Fig. 8 Equal-area projections of ChRM directions determined in the different mine sectors: **a** Teniente dacite porphyry, **b** mine sub-6, **c** Regimiento, and **d** Esmeralda. **e** Plot of the mean directions and confidence angles at 95%. *Open (filled) circles* are projections in the upper (lower) hemisphere

30 mT, indicating that the stable characteristic magnetization is likely carried by a significant content of single domain or pseudo-single domain grains. In order to understand the nature of NRM, ARM acquisition was performed on several samples from this drill core. There is a good correlation between ARM and NRM intensity (Fig. 10a). AF demagnetization curves of NRM and ARM are also similar (Fig. 10b). These observations indicate that the NRM is mainly a single component of magnetization and not the complex sum of antipodal magnetizations that would not compare well with univectorial ARM.

All the samples have negative inclinations, except in the depth interval 101–117 m where both polarities are observed (Figs. 9 and 11b, c). In two samples with positive inclination, the residual high coercitivity magnetization has negative inclination (Fig. 7e, f).

Drill cores SG184 and SG185 are oriented geotechnical cores. The expected normal polarity direction at 5 Ma for El Teniente is close to the dipole direction (declination, ~0°; inclination, ~−55°) since the apparent polar wander for the South American plate is less than 5°. For SG184, all the samples in the depth interval 66.95–222.45 m have the same declination around 300°, close to the expected direction when the drill core is rotated to the in situ position (Fig. 11d). In core coordinates, there is no significant dispersion in the magnetic inclination (Table 1, Fig. 11a). The dispersion is only observed in the declination in core coordinates and is recorded in the upper part of the core in the depth interval 37.35–55.9 m. Along the core, there is no significant

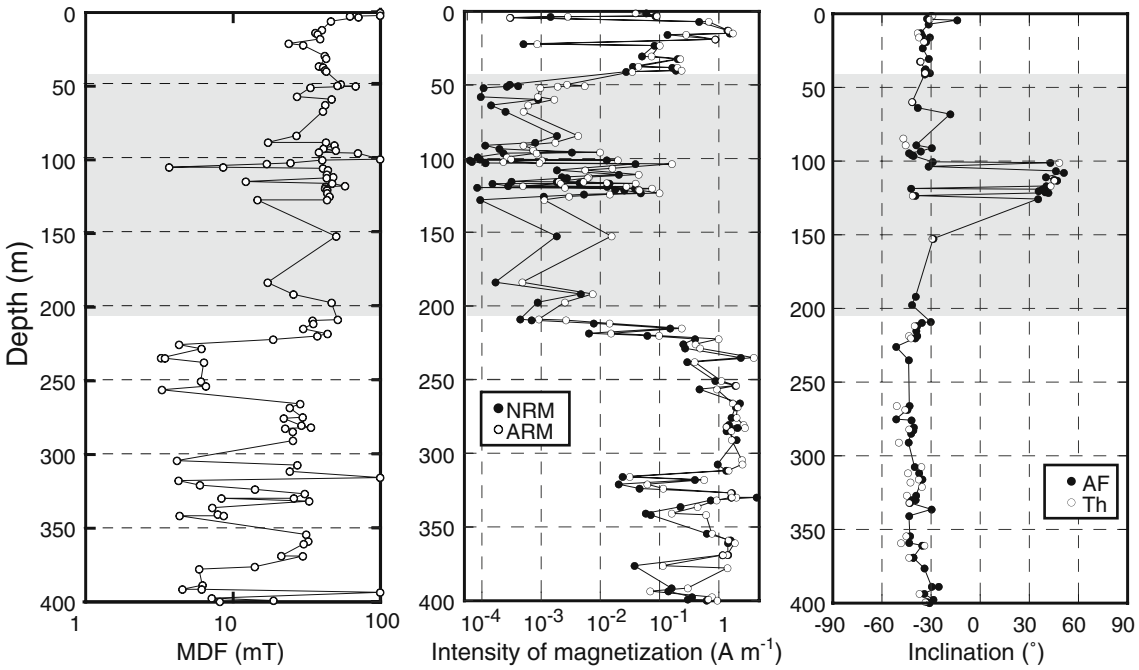

Fig. 9 Variation of MDF values, intensity of NRM and ARM, inclination of characteristic direction in drill core coordinate versus depth for samples from drill core SG185. The characteristic directions determined after progressive thermal and AF demagnetization are respectively shown with *white* and *black circles*. Note that samples from the depth interval 100–120 m have both positive and negative inclinations

change in magnetic properties; thus, variation in declination cannot be explained by a poor magnetic record but is likely the consequence of an inaccurate orientation of the drill core (Fig. 11a). In drill core SG185, the orientation was not clearly marked in several pieces of core, and in order to have more continuous sampling, samples were taken with and without orientation. This explains the more or less random distribution of the declination in core coordinates (Fig. 11b). However, as for SG184, the scatter of inclination values is low (Table 1, Fig. 11b, c), while a significant dispersion in declination in core coordinate is observed for the oriented samples, indicating the incomplete reliability of the orientation technique for these two cores. The intersections of the two small circles provide two solutions for the in situ mean characteristic direction. One of the intersections is close to the expected direction for normal polarity directions (Fig. 11g).

Teniente volcanic complex

Characteristic directions were determined at six sites (Table 1). Magnetization is carried by magnetite with unblocking temperatures in the range 450–580°C (ESM Fig. 6). Normal polarity is observed at sites located to the west of the mine, while the two sites ET05–ET06 located to the north of the mine record a reverse polarity magnetization (Fig. 12).

Discussion

The paleomagnetic study of the mineralized units of the El Teniente deposit reveals the existence of stable, well-defined, and characteristic remanent magnetizations either of normal or reverse polarity that could correspond to (1) a TRM acquired by cooling below the Curie point of magnetite, which is the main magnetic carrier, or (2) a CRM acquired during the alteration and/or crystallization of magnetic carrier minerals or more likely related to both processes. CRM acquisition during hydrothermal alteration could lead to a complex paleomagnetic record, and one should be cautious when using natural CRM apparent polarity to infer timing of the corresponding chemical event (Cairanne et al. 2003, 2004). We will first discuss the origin of the remanent magnetization and then attempt to interpret the magnetic polarity changes with respect to the evolution of the magmatic and hydrothermal system.

Magnetic mineralogy and nature of the remanent magnetization

One of the characteristics of the El Teniente deposit is that most of the copper mineralization is hosted in rocks of the CMET, which contains relatively large proportions of magnetite mainly as a secondary mineral associated with the different phases of hydrothermal alteration. Large grains

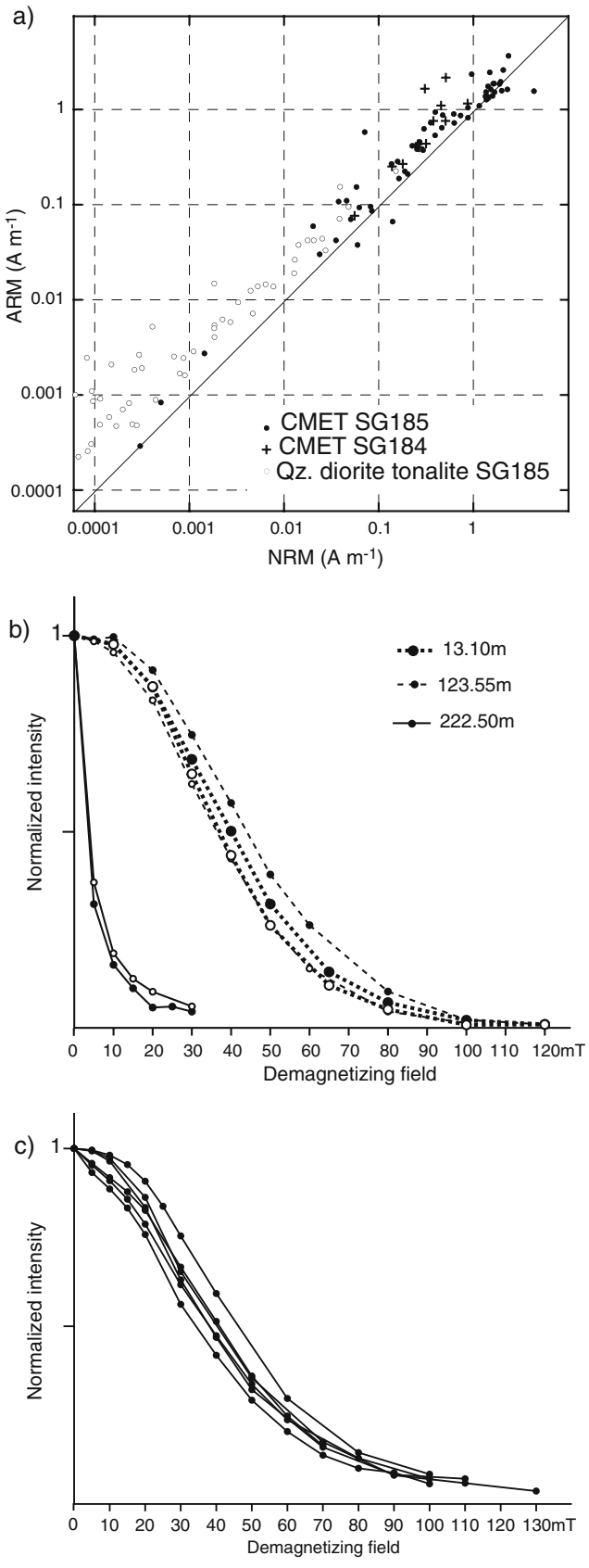

◀ **Fig. 10** **a** Log–log plot of ARM intensity versus NRM intensity for samples of drill cores SG184 and SG185. The ARM was given with a DC field of 40 μT and an AC field of 110 mT. **b** Comparison of the AF demagnetization of NRM (*filled symbols*) and ARM (*empty symbols*) for three samples of drill core SG185. **c** AF demagnetization of laboratory induced CRMs at 460°C with a DC field of 40 μT. The CRMs were given in samples from the Central quartz diorite–tonalite stock with initial low magnetic susceptibility and large increase in susceptibility upon heating above 400°C

of magnetite are common in the CMET and are usually associated with biotitization (Fig. 4c, d), contributing to a high magnetic susceptibility. Some samples do not show the association of magnetite–biotite but have a large number of smaller magnetite grains distributed either in the groundmass (Fig. 4b) or within plagioclase crystals (Fig. 4a). Optical observations (Fig. 4a) and backscattered SEM images reveal the existence of numerous small magnetite grains (<10 μm) often located within plagioclase crystals (Fig. 4g–i). Pyrrhotite or other magnetic minerals were not observed and have not been reported at El Teniente.

In rock magnetism, large magnetite crystals are multi-domain grains that are unlikely to record a significant stable remanent magnetization. On the other hand, titanomagnetite inclusions in pyroxene and plagioclase crystals of mafic intrusive and metamorphic rocks have been known to record stable magnetizations consistent with expected geomagnetic field orientations (Evans and McElhinny 1966; Hargraves and Young 1969; Renne et al. 2002; Feinberg et al. 2005, and references herein). The hosting silicate mineral isolates these magnetic inclusions against chemical alteration by hydrothermal fluids and protects the titanomagnetite from oxidation. In a Cu–porphyry deposit like El Teniente, hydrothermal alteration is, however, likely to involve high temperature magmatic hydrothermal fluids capable of altering the silicate host minerals. Although some of the magnetite crystals may have been incorporated in plagioclase crystals during the crystallization of plagioclase, Skewes et al. (2005) and Cannell et al. (2005) attribute the formation of these magnetite crystals to an early phase of alteration prior to the late magmatic alteration phase carrying the main mineralization. Taking into account the high unblocking temperatures of magnetite, the magnetization of the smallest grains within the plagioclase could thus be contemporaneous with the pre-mineralization alteration phase. However, the same highly stable magnetization was observed in samples without and with large chalcopyrite veins (Fig. 3), and this observation suggests that any magnetization acquired prior to the formation of the mineralized veins was almost totally reset by the circulation of hot fluids (>400°C). We speculate that the stable magnetization was recorded during copper mineralization and likely postdates the formation of magnetite in plagioclase crystals. In rocks of the CMET,

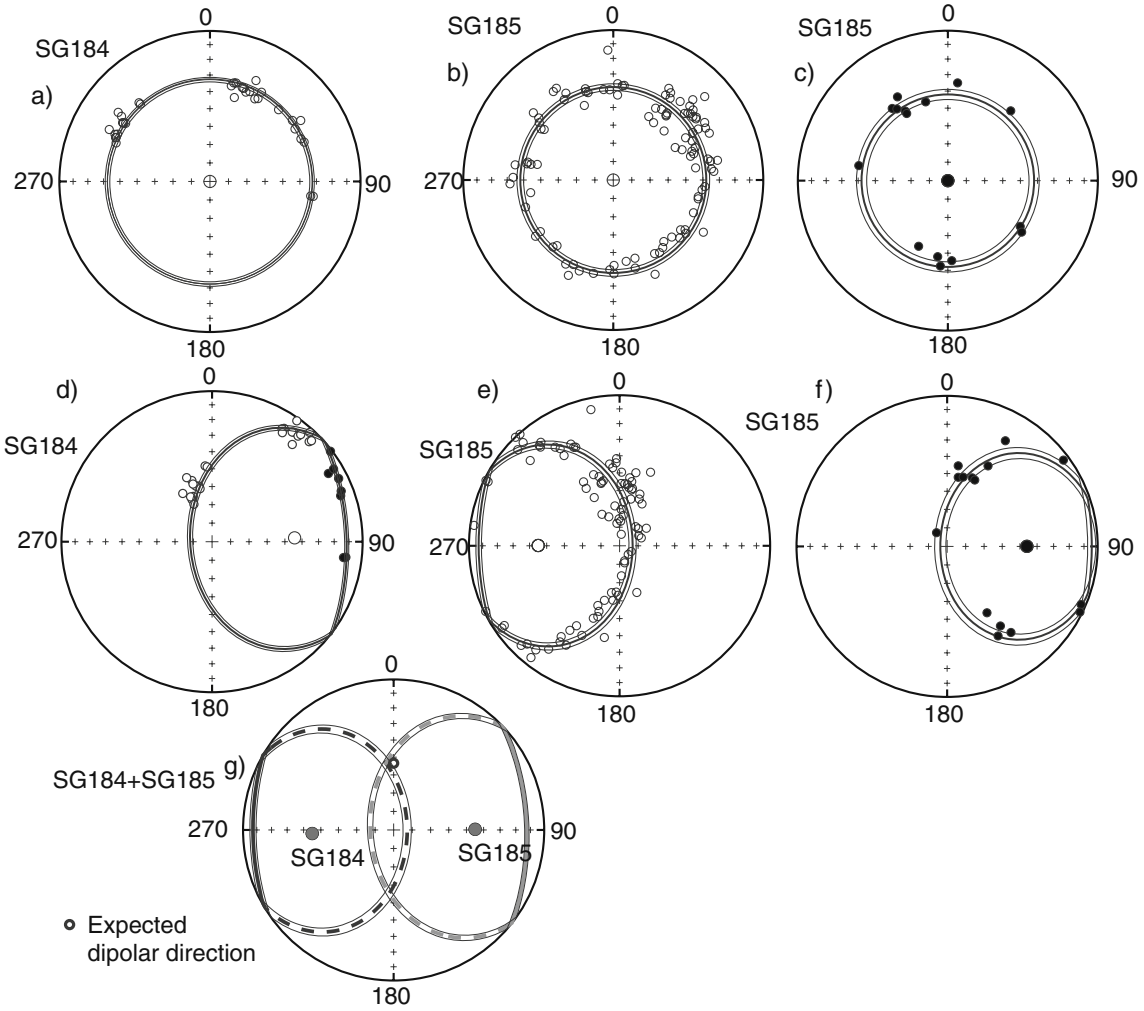

Fig. 11 Equal-area projection of characteristic magnetizations in drill core coordinates (**a** samples from drill core SG184; **b**, **c**, samples with normal (reverse) polarity from drill core SG185; **d**–**f** same as **a**–**c** with the drill core rotated). **g** Plot of the *two small circles* determined from the mean inclination of the characteristic magnetizations of normal polarity and plotted after rotation of the drill cores. The most likely common direction of ChRM in both drill cores is likely the intersection close to the expected direction

the magnetic carrier is magnetite with unblocking temperatures in the range of 500–580°C and MDF values in the range of 30–40 mT. Within the El Teniente deposit and especially within the CMET, the main magnetic difference between samples with similar magnetic properties is the change in magnetic polarity spatially within the deposit. For example, samples from the CMET with fine-grained magnetite crystals record normal polarity in the drill cores, but a reverse polarity is observed in the Teniente sub-6 mine sector, samples having the same apparent alteration or lithologic mineral association.

We interpret that the initial magnetization of the CMET, if any, was likely fully reset. Because several geomagnetic polarity reversals occurred during the estimated time interval of magmatic and hydrothermal alteration at El Teniente (~6.5–4.5 Ma), samples from the CMET should have been altered during successive normal and reverse polarity time intervals, and magnetization within a sample should represent a complex sum of normal and reverse polarity magnetization. Except for a few samples from drill core SG185 where there is some evidence for a component of magnetization of opposite polarity after AF demagnetization at 100 mT, there is no evidence during AF or thermal demagnetization for superimposed dual polarity magnetization within the samples. NRM intensity is also comparable to ARM intensity in a laboratory field of 40 μT (Fig. 10a), and NRM and ARM behave similarly upon AF demagnetization. These experiments suggest that variations in NRM intensities between samples are mainly controlled by changes in content and nature of magnetic mineralogy rather than the result of superimposed magnetization overprints of opposite polarities.

In drill core SG185, a complex pattern of reverse and normal polarity magnetizations is, however, observed in a

Table 1 Paleomagnetic results

Site	*N*	In situ				Tilt corrected			
		Dec	Inc	α95	k	Dec	Inc	α95	k
Outside the mine : Teniente volcanic complex									
ET02	9	355.5	−45.9	7.1	53	19.0	−55.5	6.1	71
ET03	5	353.9	−50.2	4.0	361	353.9	−50.2	4.0	361
ET04	11	345.3	−71.4	9.5	23	350.8	−63.7	9.5	23
ET05	10	192.9	63.1	3.5	188	192.9	63.1	3.5	18
ET06	9	190.2	57.5	4.2	149	190.2	57.5	4.2	149
ET08	10	11.9	−61.1	3.8	158	11.9	−61.1	3.8	158
Mean	6	1.7	−58.6	9.0	57	6.4	−58.9	6.5	106
Within the mine									
Esmeralda	10	358.9	−48.0	9.2	28				
TDP	13	164.3	61.0	11.5	13				
Sub-6	17	177.4	61.2	6.2	34				
Regimiento	8	184.0	53.6	6.1	83				
Regimiento	18	5.6	−54.3	7.7	21				
Mean	5	358.6	−55.8	6.8	128				
Expected		356.3	−55.3						
Drill cores									
SG185 (*R*)	15		42.0	3.0	159				
SG185 (*N*)	102		−38.0	1.6	79				
SG184 (*N*)	33		−32.6	1.4	325				

The mean inclination for a drill core is given in drill core coordinate

N number of samples, *Dec* declination, *Inc* inclination, *α95* semi angle of confidence, *k* Fisher concentration parameter, *TDP* Teniente dacite porphyry

very short depth interval in the center of the intrusive where a large fragment of mafic rocks is reported at 106 m. The magnetic properties of the samples with opposite polarities are, however, not significantly different, and they all share the same apparent lithology and alteration.

Preliminary experiments of laboratory-induced CRM were performed on several samples, which were heated in air up to 450°C and held at that temperature during 3 h. Samples from the mafic complex without magnetic susceptibility changes during heating do not record significant CRM. However, samples from the Teniente dacitic porphyry and the quartz diorite–tonalite stocks with a 10- to 20-fold increase in magnetic susceptibility record a strong CRM (about 0.1 A/m). When the experiment is repeated at 460°C with the samples rotated 90° with respect to the applied laboratory field, a new CRM is recorded, removing nearly two thirds of the previous CRM. The laboratory-acquired CRMs present the same magnetic stability versus AF demagnetization than the ARM and the NRM (Fig. 10c). Although it is not possible to extrapolate laboratory experiments, these experiments demonstrate that CRM acquisition at temperature lower than the Curie point could be significant enough to reset partially or totally previous magnetizations and produce a complex pattern of polarity as the one observed in samples from the altered Central quartz diorite–tonalite in drill core SG185.

There are two alternative interpretations to the apparent record of a unique polarity in the samples from the CMET. One possibility is that mineralization and cooling were

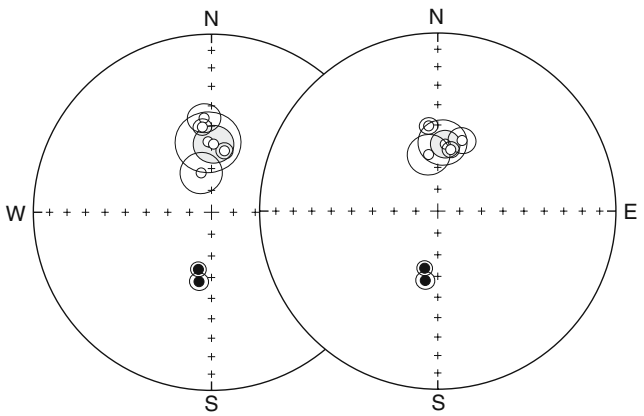

Fig. 12 Equal-area projections of ChRM directions with the 95% confidence angle determined at six sites (*left* in situ, *right* tilt corrected). *Open (filled) circles* are projections in the upper (lower) hemisphere. The mean is highlighted with the cone of confidence in *gray*

rapid enough to enable only the record of one polarity in these samples. The second interpretation is that the polarity of CRM magnetization corresponds mainly to the main polarity interval during the chemical reactions leading to the formation of new secondary magnetite or transformation of primary magnetite grains or the last polarity interval prior to cooling to lower temperature. Sulfur isotope geothermometry from El Teniente indicates a sulfide deposition temperature of 456±41°C during the potassic alteration (Kusakabe et al. 1984). Recent studies of ∂18O and ∂D in Cu porphyry deposits indicate the dominant role of magmatic over meteoric fluids with the consequence of high temperature alteration for both the early potassic and main-stage phyllic alteration with temperatures from 600°C to 550°C (Harris and Golding 2002). Stern et al. (2007) report high temperatures (>600°C) calculated from oxygen isotopes of quartz–magnetite and magnetite–anhydrite mineral pairs within the A porphyry microdiorite, but a lower range of temperatures (455–495°C) was determined from sulfur isotopes. Microthermometric data for fluid inclusions from Klemm et al. (2007) indicate that copper sulfides precipitated upon cooling between 410°C and 320°C. We can thus speculate that the temperature of the hydrothermal fluids was sufficiently high (>450°C) to reset any previous magnetization in the CMET unit and that the NRM is likely a combination of CRM and TRM acquired during mineralization and cooling.

Magnetic polarity zonation within the deposit

Maksaev et al. (2004) interpret molybdenite Re–Os dating at El Teniente as evidence for ore deposition at 6.30±0.03, 5.60±0.02, 5.01 to 4.96, 4.89±0.08 to 4.78±0.03, and 4.42±0.02 Ma, concurrent with five intrusive episodes, and suggest that the Re–Os system for molybdenite was unaffected by various hydrothermal episodes. The same authors suggest that the $^{40}Ar/^{39}Ar$ system of micas was reset by high-temperature (>350°C) fluid circulation and provides only a partial record of the latest history of development of this ore-forming system; biotite, sericite, and altered whole-rock samples collected throughout the ore body yielded 40 $^{40}Ar/^{39}Ar$ plateau ages ranging from 5.06±0.12 to 4.37±0.10 Ma.

In the Teniente dacite porphyry, the less altered samples record a well-defined reverse polarity magnetization that is interpreted to represent the cooling of the Teniente dacite porphyry. All the samples with a stable characteristic magnetization nearby the Teniente dacite porphyry have also the reverse component of magnetization. The same behavior is observed in the Teniente sub-6 mine sector. While a U–Pb age of 5.28±0.10 Ma is obtained on zircon of the Teniente dacite porphyry, $^{40}Ar/^{39}Ar$ ages on biotite and sericite are not statistically different and provide a mean age of 4.67±0.07 Ma. A similar age is also found in the biotitized CMET (samples TT-15 and TT-56 from Maksaev et al. 2004).

In the Regimiento sector to the southwest of the Braden breccia pipe (Fig. 2), a normal polarity is observed near the breccia pipe, but a reverse polarity is found at one location (samples TR07–TR11, ESM Fig. 1e).

Within the two analyzed drill cores, a normal polarity is observed except within the center of the quartz diorite–tonalite stock in drill core SG185. The two drill cores SG184 and SG185 are located near or across the Central quartz diorite–tonalite. The spread in U–Pb ages in the Sewell, Northern, and Central quartz diorite–tonalite stocks was interpreted to represent partial Pb loss produced by potassic hydrothermal overprint at 5.67–5.48 Ma. Maksaev et al. (2004) separated arbitrarily the U–Pb spot ages into two groups of U–Pb ages (~6.3±0.15 and ~5.6±0.1 Ma) for the Sewell stock and the Central quartz diorite–tonalite. The youngest U–Pb ages are not different from $^{40}Ar/^{39}Ar$ ages in unaltered magmatic biotite crystals from the Sewell stock, but the $^{40}Ar/^{39}Ar$ ages in hydrothermal biotite and sericite crystals are significantly younger and are not statistically different from those observed in the Braden breccia pipe or around the Teniente dacite porphyry.

There is a systematic difference between the U–Pb ages and the $^{40}Ar/^{39}Ar$ ages in hydrothermal biotite and sericite crystals. For the Teniente dacite porphyry, the difference is of ~0.6 Ma and up to 1 Ma for the Sewell stock. Such differences are interpreted to represent the time of cooling of the hydrothermal system from about ~800°C (closure of the U–Pb system) to ~300±50°C (closure of the argon system) (Harrison et al. 1985). Blocking of the remanent magnetization likely occurred in a temperature interval bounded by the Curie point of magnetite (580°C) and about 350–400°C associated with sulfide deposition and CRM acquisition. When compared with the geomagnetic reversal polarity time scale, the reverse polarity of the Teniente dacite porphyry thus implies that cooling below 580°C should have occurred either from 5.28 to 5.235 Ma, from 4.997 to 4.89 Ma, or in the time interval 4.799–4.631 Ma when the earth's magnetic field was of reverse polarity (Fig. 13). This last interval is in agreement with the mean $^{40}Ar/^{39}Ar$ ages reported in the northern part of the deposit.

There is no evident interpretation of the normal polarity encountered in the Esmeralda, Regimiento, and drill core samples, except that the acquisition of the magnetization cannot be associated with an eventual hydrothermal event related to the intrusion of the Teniente dacite porphyry. In the time interval 4–6.5 Ma, the normal polarity intervals have a length of 97–238 ka. The tentative correlation of magnetic polarities with the isotopic ages is also hampered by uncertainties in the absolute ages. Significant time differences (~1 Ma) between U–Pb ages and $^{40}Ar/^{39}Ar$

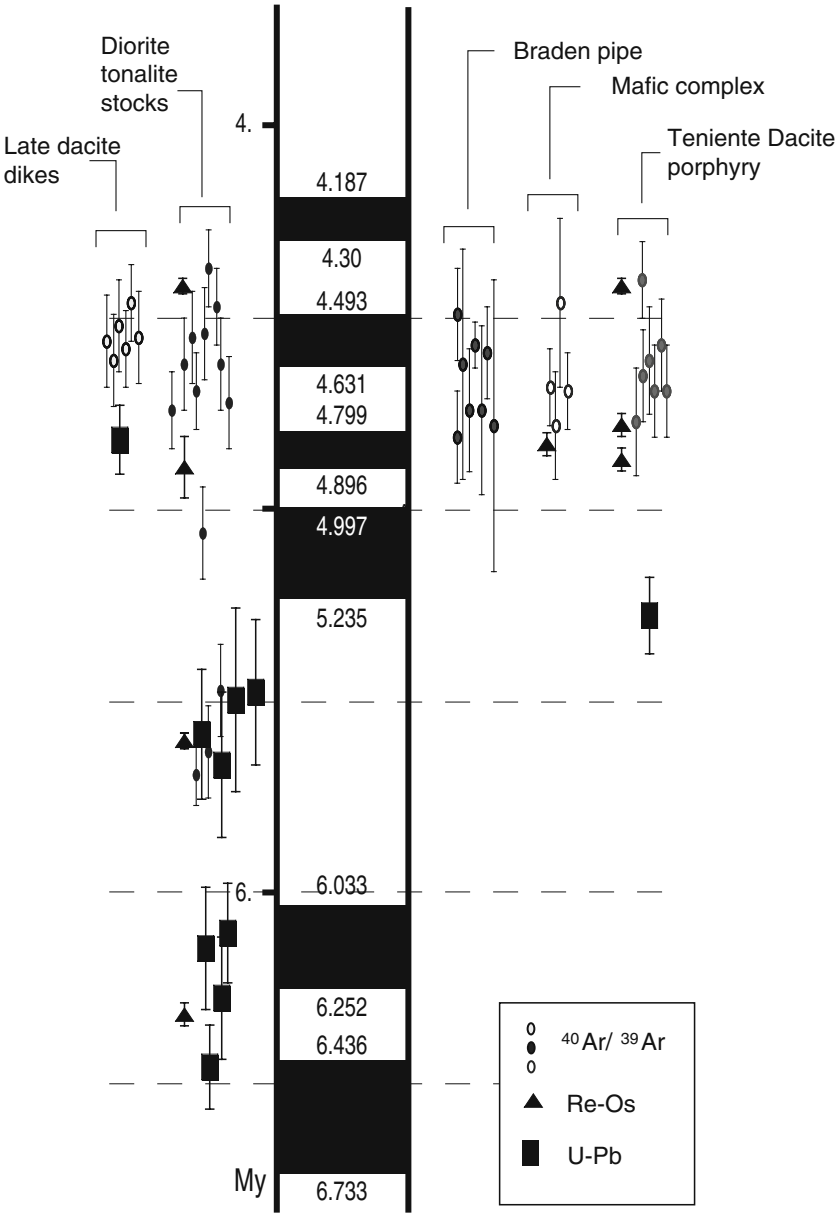

Fig. 13 Plot of the radiometric ages obtained for different rock units at El Teniente (Maksaev et al. 2004). *Circles*, *rectangles*, and *triangles*, respectively, correspond to $^{40}Ar/^{39}Ar$, U–Pb, and Re–Os ages. U–Pb and Re–Os ages in the quartz diorite–tonalite intrusions from Maksaev et al. (2004). Geomagnetic polarity time scale (Gradstein et al. 2004)

ages determined by laser step heating of biotite on the same intrusions have been often reported, indicating that the U–Pb ages may not always correspond to the time of emplacement, as in the case suggested by Halter et al. (2005) for the oldest intrusive stocks in the Alumbrera deposit (Harris et al. 2004, 2008).

Skewes et al. (2005) and Skewes and Stern (2007) suggest that there is an intimate spatial and temporal association of different stages of mineralization at El Teniente with the emplacement of multiple hydrothermal breccia complexes and that mineralization was not emplaced by the small diorite–tonalite stocks and the Teniente dacite porphyry. Although a more systematic paleomagnetic sampling is needed to map magnetic polarity changes within the mine, preliminary data here presented are in better agreement with magmatic hydrothermal processes associated with diorite–tonalite stocks and the Teniente dacite porphyry as suggested by results nearby the porphyry or in the sub-6 mine sector.

In drill core SG185, samples from the mafic rocks within a few meters of the Central quartz diorite–tonalite stock record a very stable remanent magnetization that demonstrates that the characteristic magnetization is acquired during the mineralization associated with the intrusion of this stock, supporting the interpretations from Cannell et al. (2007) that brecciation occurred either synchronously with or after tonalitic–dioritic magmatism. Finally, the complex polarity pattern in the center of the Central quartz diorite–tonalite sampled in drill core SG185 (Fig. 9c) is likely related to the very low magnetic signal in these rocks, more easily affected by a localized late alteration event. In

contrast, the strong magnetic signal in rocks of the CMET associated with large contents of magnetite as shown by the high magnetic susceptibility is probably less affected by these late alteration events.

The mean direction calculated for the sites inside and outside the mine is close to the expected direction at 5 Ma (Figs. 8e, 11g, and 12). There is no paleomagnetic evidence for a tilt or tectonic rotation of the El Teniente district. This observation is in good agreement with the lack of evidence for significant displacement (>40 m) along the main faults observed within the mine and the main activity of the TFZ ended before the emplacement of the intrusions and mineralization (Garrido et al. 2002).

Conclusions

Despite the presence of a large amount of multidomain magnetite, a stable characteristic remanent magnetization with high unblocking temperatures is observed. MDFs above 30 mT in most samples indicate that pseudo-single domain or single domain grains carry the remanent magnetization. Very fine-grained magnetite is indeed observed especially in plagioclase affected by an early Na–Ca–Fe alteration.

Radiometric dating suggests a period of hydrothermal activity, which extended either continuously or episodically, for at least 0.69±0.22 Ma and that comprises a succession of episodes of ore deposition. The present paleomagnetic study shows NRM of both polarities in agreement with a time interval of mineralization encompassing several polarity reversals. However, most if not all of the samples show evidence for a dominant magnetization of either polarity with well-defined spatial distribution rather than a complex pattern of dual-polarity magnetizations within a sample or between nearby samples. For example, the Teniente dacite porphyry, associated breccias, and nearby mineralized mafic rocks record a reverse polarity magnetization. In contrast, a normal polarity magnetization is systematically observed in the CMET samples of the two long drill cores SG184 and SG185. The apparent complete reset of the remanent magnetization carried by fine-grained magnetite included in plagioclase crystals indicates temperatures of the magmatic fluids above or near the Curie point of magnetite (580°C). The lack of evidence of successive magnetic overprints by different episodes of ore deposition can be interpreted as evidence for spatially localized short-lived events of mineralization. The duration of the localized hydrothermal events is constrained by the short duration (~100 ka) of the normal polarity magnetic subchrons in the time interval (5.06±0.12 to 4.37±0.10 Ma). A systematic mapping of the remanent magnetization using the numerous diamond cores drilled at El Teniente would help understand the spatial and temporal evolution of this giant deposit.

The paleomagnetic evidence, together with geochronological evidence presented by Maksaev et al. (2004), indicate that a simplified four-stage model for El Teniente, divided in (1) late magmatic, (2) main hydrothermal, (3) late hydrothermal, and (4) posthumous stage, as presented by Cuadra (1986) and Arevalo et al. (1998), remains but a broad simplification that does not recognize various short lived single mineralization events, some superimposed and some distinctly separated in time and space. Multiple mineralization events, each one with its own evolution stages, superimposed within the district, may explain the polarity zonation as well as the gigantism of the deposit. The El Teniente supergiant porphyry copper deposit represents the sum of multiple smaller porphyry copper systems, these having evolved separated in time and space and in some cases superimposed.

Acknowledgments We would like to thank the "Superintendencia de Geologia El Teniente" for their logistical support for sampling within the mine. Ludovina Burgos and other geologists from El Teniente are thanked for assistance for sampling the drill cores and discussion about the El Teniente geology. Reviews by F. Tornos, A. Rapalini, and an anonymous reviewer significantly improved the manuscript. We thank Andres Tassara and Miguel Faundez for their help during the initial stages of this project. Original work was financed by project DID-I009-99/2, University of Chile, and IRD, France.

References

Alva-Valdivia LM, Rivas M, Goguitchaichvili A, Urrutia-Fucugauchi J, Gonzalez JA, Vivallo W (2003) Integrated magnetic studies of the El Romeral iron-ore deposit, Chile: implications for ore genesis and modeling of magnetic anomalies. J Appl Geophys 53:137–151

Arevalo A, Floody R, Olivares A (1998) Modelo Geometalúrgico. Estudio geometalúrgico del mineral a explotar a mediano y largo plazo, Superintendencia Geología de El Teniente, CODELCO-CHILE, Int Report GL-133/98

Burgos L (2002) Petrografía y Geoquímica de la Diabasa y Diques Basálticos que constituyen las "Andesitas de la Mina" en el yacimiento El Teniente, VI región, Chile. Thesis, Departamento de Ciencias de la Tierra, Universidad de Concepción, pp 108

Butler R (1992) Paleomagnetism: magnetic domains to geologic terranes. Blackwell, Oxford, p 336

Cairanne G, Brunet F, Pozzi JP, Besson P, Aubourg C (2003) Magnetic monitoring of nucleation and growth of magnetite: the record of magnetic reversal. Am Mineral 88:1385–1389

Cairanne I, Aubourg C, Pozzi JP, Moreau M-G, Decamps T, Marolleau G (2004) Laboratory chemical remanent magnetization in a natural claystone: a record of two magnetic polarities. Geophys J Int 159:909–916

Camus F (1975) Geology of the E1 Teniente orebody with emphasis on wall–rock alteration. Econ Geol 70:1341–1372

Cannell J, Cooke D, Walshe J, Stein H (2005) Geology, mineralization, alteration, and structural evolution of the El Teniente porphyry Cu–Mo deposit. Econ Geol 100:979–1003

Cannell J, Cooke D, Walshe J, Stein H (2007) Geology, mineralization, alteration, and structural evolution of the El Teniente porphyry Cu-Mo deposit—a reply. Econ Geol 102:1071–1190

Cathles LM, Erendi AHJ, Theyer JB, Barrie CT (1997) How long can a hydrothermal system be sustained by a single intrusion event? Econ Geol 92:766–771

Courtillot V, Féraud G, Maluski H, Vandamme D, Moreau MG, Deccan BJ (1988) Flood basalts and the cretaceous/tertiary boundary. Nature 333:843–846

Cuadra P (1986) Geocronología K-Ar del yacimiento El Teniente y áreas adyacentes. Rev Geol Chile 27:3–26

Deckart K, Clark AH, Aguilar AC, Vargas RR, Bertens NA, Mortensen JK, Fanning M (2005) Magmatic and hydrothermal chronology of the giant Rio Blanco porphyry copper deposit, central Chile; implications of an integrated U–Pb and $^{40}Ar/^{39}Ar$ database. Econ Geol 100:905–934

Dilles JH, Einaudi MT (1992) Wall-rock alteration and hydrothermal flow paths about the Ann-Mason porphyry copper deposits, Nevada—a 6-km vertical reconstruction. Econ Geol 87:1963–2001

Evans ME, McElhinny MW (1966) The paleomagnetism of the Modipe gabbro. J Geophys Res 71:6053–6063

Feinberg JM, Scott GR, Renne PR, Wenk H-R (2005) Exsolved magnetite inclusions in silicates: features determining their remanence behavior. Geology 33:513–516

Garrido I, Riveros M, Cladouhos T, Espieira D, Allmendinger R (1994) Modelo geológico estructural yacimiento El Teniente. Proceedings, VII Congreso Geológico Chileno, Concepción 2, pp 1553–1558

Garrido I, Cembrano J, Siña A, Stedman P, Yañez G (2002) High magma oxidation state and bulk crustal shortening: key factors in the genesis of Andean porphyry copper deposits, central Chile (31–34°S). Rev Geol Chile 29:43–54

Goguitchaichvili A, Chauvin A, Roperch P, Prevot M, Aguirre L, Vergara M (2000) Paleomagnetic results from the Miocene Farellones formation: a possible highest paleosecular variation during the Miocene. Geophys J Int 140:357–373

Gradstein FM, Ogg JG, Smith AG et al (2004) A geologic time scale 2004. Cambridge University Press, Cambridge, p 589

Halter WE, Heinrich CA, Pettke T (2005) Magma evolution and the formation of porphyry Cu–Au ore fluids: evidence from silicate and sulfide melt inclusions. Miner Deposita 39:845–863

Hargraves RB, Young WM (1969) Source of stable remanent magnetism in Lambertville diabase. Am J Science 267:1161–1177

Harris AC, Golding SD (2002) New evidence of magmatic-fluid-related phyllic alteration: Implications for the genesis of porphyry Cu deposits. Geology 30:335–338

Harris AC, Allen CM, Bryan SE, Campbell IH, Holcombe RJ, Palin JM (2004) ELA-ICP-MS U–Pb zircon geochronology of regional volcanism hosting the Bajo de la Alumbrera Cu-Au deposit: implications for porphyry-related mineralization. Miner Deposita 39:46–67

Harris AC, Dunlap WJ, Reiners P, Allen CM, Cooke DR, White NC (2008) Multimillion year thermal history of a porphyry copper deposit: application of U–Pb, 40Ar/39Ar and (U–Th)/He chronometers, Bajo de la Alumbrera copper–gold deposit, Argentina. Miner Deposita 43:295–314

Harrison TM, Duncan I, McDougall I (1985) Diffusion of ^{40}Ar in biotite; temperature, pressure and compositional effects. Geochim Cosmochim Acta 49:2461–2468

Hedenquist JW, Richards JP (1998) The influence of geochemical techniques on the development of genetic models for porphyry copper deposits. In: Richards JP, Larson PB (eds) Techniques in hydrothermal ore deposits. Rev Econ Geol 10:235–256

Klemm LM, Pettke T, Heinrich CA, Campos E (2007) Hydrothermal evolution of the El Teniente deposit, Chile: porphyry Cu-Mo ore deposition from low-salinity magmatic fluids. Econ Geol 102: 1021–1045

Kusakabe M, Nakagawa S, Hori M, Matsuhisa Y, Ojeda JM, Serrano L (1984) Oxygen and sulfur isotopic composition of quartz, anhydrite and sulfide minerals from the El Teniente and Rio Blanco porphyry copper deposits, Chile. Bull Geol Soc Japan 35:583–614

Lindgren W, Bastin ES (1922) Geology of the Braden mine, Rancagua, Chile. Econ Geol 17:863–905

Maksaev V, Munizaga F, McWilliams M, Fanning M, Mathur R, Ruiz J, Zentilli M (2004) New chronology for El Teniente, Chilean Andes, from U–Pb, $^{40}Ar/^{39}Ar$, Re–Os and fission-track dating: implications for the evolution of a supergiant porphyry C-Mo deposit. Soc Econ Geol Spec Publ 11:15–54

Ossandón G (1974) Petrografía y alteración del pórfido dacítico, yacimiento El Teniente. Thesis, Departamento de Geología, Universidad de Chile, Santiago, pp 116

Padilla-Garza RA, Titley SR, Eastoe CJ (2004) Hypogene evolution of the Escondida porphyry copper deposit, Chile. Soc Econ Geol Spec Publ 11:141–165

Palfy J, Mundil R, Renne PR, Bernor RL, Kordos L, Gasparik M (2007) U–Pb and $^{40}Ar/^{39}Ar$ dating of Miocene fossil track site at Ipolytarnoc (Hungary) and its implications. Earth Planet Sci Lett 258:160–174

Reid MR, Coath CD, Harrison TM, McKeegan KD (1997) Prolonged residence times for the youngest rhyolites associated with Long Valley Caldera: ^{230}Th-^{238}U ion microprobe dating of young zircons. Earth Planet Sci Lett 150:27–39

Renne PR, Scott GR, Glen JMG, Feinberg JM (2002) Oriented inclusions of magnetite in clinopyroxene: source of stable remanent magnetization in gabbros of the Messum Complex, Namibia. Geochem Geophys Geosys 3(12):1079

Seedorff E, Dilles JH, Profett JM, Einaudi MT, Zurcher L, Stavast W, Johnson DA, Barton MD (2005) Porphyry deposits: characteristics and origin of hypogene features. Econ Geol 100th Anniversary Volume, pp 251–298

Skewes A, Stern CR (2007) Geology, mineralization, alteration, and structural evolution of the El Teniente Porphyry Cu-Mo deposit—a discussion. Econ Geol 102:1171–1180

Skewes A, Arévalo A, Floody R, Zuñiga P, Stern CR (2002) The giant El Teniente breccia deposit: hypogene copper distribution and emplacement. In: Goldfarb RJ, Nielsens RL (eds) Integrated methods for discovery: global exploration in the twenty-first century. Soc Econ Geol Spec Publ 9, pp 299–332

Skewes MA, Arévalo A, Floody R, Zuñiga P, Stern CR (2005) The El Teniente megabreccia deposits, the world's largest copper deposit. In: Porter TM (ed) Super porphyry copper & gold deposits-a global perspective, 1. PGC, Adelaide, pp 83–113

Stern CR, Funk J, Skewes A, Arevalo A (2007) Magmatic anhydrite in plutonic rocks at The El Teniente Cu–Mo deposit, Chile, and the role of sulfur- and copper-rich magmas in its formation. Econ Geol 102:1335–1344

Symons D, Arne D (2005) Paleomagnetic constraints on Zn–Pb ore genesis of the Pillara Mine, Lennard Shelf, Western Australia. Miner Deposita 39:944–959

Symons D, Smethurst M, Ashton JH (2002) Paleomagnetism of the Navan Zn–Pb deposit, Ireland. Econ Geol 97:997–1012

Tauxe L, Butler R, Banerjee SK, van der Voo R (2009) Essentials of paleomagnetism. University of California Press, Berkeley, pp 504

Townley B, Roperch P, Oliveros V, Tassara A, Arriagada C (2007) Hydrothermal alteration and magnetic properties of rocks in the Carolina de Michilla Stratabound Copper District, Northern Chile. Miner Deposita 42:771–789

Villalobos J (1975) Alteración hidrotermal en las andesitas del yacimiento El Teniente, Chile. Thesis, Departamento de Geología, Universidad de Chile, pp 125

Zuñiga P (1982) Alteración y mineralización hipógenas en el sector oeste del yacimiento El Teniente. Thesis, Departamento de Geología y Geofísica, Universidad de Chile, pp 104